Non Destructive Testing techniques based on nonlinear methods for assessment of debonding in single lap joints

G. Scarselli*[a], F. Ciampa[b], D. Ginzburg[b], M. Meo[b]
[a]Department of Engineering for Innovation, University of Salento,
Via per Monteroni (Lecce), 73100, Italy
[b]Material Research Centre, Department of Mechanical Engineering,
University of Bath, Bath, BA2 7AY, UK

ABSTRACT

Nonlinear ultrasonic non-destructive evaluation (NDE) methods can be used for the identification of defects within adhesive bonds as they rely on the detection of nonlinear elastic features for the evaluation of the bond strength. In this paper the nonlinear content of the structural response of a single lap joint subjected to ultrasonic harmonic excitation is both numerically and experimentally evaluated to identify and characterize the defects within the bonded region. Different metallic samples with the same geometry were experimentally tested in order to characterize the debonding between two plates by using two surface bonded piezoelectric transducers in pitch-catch mode. The dynamic response of the damaged samples acquired by the single receiver sensor showed the presence of higher harmonics (2^{nd} and 3^{rd}) and subharmonics of the fundamental frequencies. These nonlinear elastic phenomena are clearly due to nonlinear effects induced by the poor adhesion between the two plates. A new constitutive model aimed at representing the nonlinear material response generated by the interaction of the ultrasonic waves with the adhesive joint is also presented. Such a model is implemented in an explicit FE software and uses a nonlinear user defined traction-displacement relationship implemented by means of a cohesive material user model interface. The developed model is verified for the different geometrical and material configurations. Good agreement between the experimental and numerical nonlinear response showed that this model can be used as a simple and useful tool for understanding the quality of the adhesive joint.

Keywords: debonding, damage detection, nonlinear elastic wave spectroscopy, kissing bond

1. INTRODUCTION

Structural health monitoring (SHM) systems based on ultrasonic wave propagation are able to provide information about the structural characteristics and the residual life of a component. These methods can improve safety and reduce maintenance costs. However, one of the major limiting factors in the use of current ultrasonic SHM methods for adhesive bonding is their capability to quantitatively detect and evaluate defects in the joint, particularly in the interfacial region between substrate and adhesive layer. Indeed, manufacturing errors and operating conditions (exposure of joints to moisture and temperature changes in service) can lead to the degradation of bonded joints resulting in their loss of strength and alteration of their mechanical properties. This degradation often results in a change of the adhesive elastic modulus. Defects in adhesive joints can be classified into three broad categories, i.e. internal gross defects, cohesive defects and adhesive defects. Conventional ultrasonic techniques are not so effective in detecting poor adhesion between the adhesive and the substrate as this thin interfacial layer could be orders of magnitude less than the wave length used [1-4]. These defects are often termed kissing bonds or zero volume bonds, where the two surfaces are held together by a compressive stress with no molecular forces acting between them. In [5] a kissing bond is defined as a perfect contact between two surfaces which transmits no shear stress. A number of scientific papers are available in literature on kissing bonds because the combination of severity and detection difficulty of this type of defects in an adhesively bonded structure makes it of significant practical importance. If an adhesive joint consisting of two adherends undergoes a higher loading than estimated or a fault during the production process is involved, the consequence may be a damage within the glue layer or directly at the interface of the adherend. This bonding problem is in fiber-reinforced technology sometimes erroneously denoted as delamination, which is generally a separation between laminate layers. The effect of weak bonds is that they can result in sudden and unexpected failures of the bonded joints. The main issue in the

*gennaro.scarselli@unisalento.it: phone 0039 0832299720; fax 0039 0832299919; www.dii.unisalento.it

detection of this type of defects is that a weak bond with a low elastic modulus can show nearly the same behavior in a non-destructive testing (NDT) procedure respect to a perfect one. When a kissing bond appears, surrounded by a well-bonded area, sufficient compressive residual stress at the adherend-adhesive interface makes the flaw invisible for many conventional nondestructive testing methods such as ultrasounds. In [6] digital image correlation (DIC) has been used to detect and evaluate kissing bonds and the main finding is that digital image correlation technique could detect the kissing bonds even at 50% of the failure load. The main downside of this method is that it requires a heavy experimental effort and fall outside the category of the possible SHM approaches. In [7] structures with lap splice joints have been investigated for the purpose of guided-wave-based debonding damage detection. Fiber optic Doppler (FOD) sensors were used to acquire guided ultrasonic waves propagating in aluminum and CFRP bonded assemblies. A self-calibration sensor network configuration was proposed in order to measure both the baseline and the damage-related signals during single excitation. The most distinct and simplest signal feature, namely the arrival time of the first wave package, was extracted and applied to identify disbonds in the lap splice joint of the specimens. The basic principle of this technique is that disbonds delay the arrival time of the debonding-related guided wave signals in comparison with the baseline measurements. Different inspection methods applied on sets of weak bond specimens are described in [8]. The authors stated that one NDT method may not detect all types of weak bonds. The inspection techniques have to be highly sensitive in order to differentiate the subtle differences between optimum bonds and weak bonds. The adhesive itself plays an important role and it is also the combination with different adherent materials which causes problems. For instance, lock-in thermography with ultrasonic excitation is a successful tool for detecting many bonding defects but it fails solving the kissing bond problem with a desired reliability. The numerous literature sources evaluated in [9] clearly confirms that the adhesive bond quality is a critical parameter that cannot yet be assessed by any NDT techniques. Several conventional methods are suitable and improved for a better detection capability but, up to day, no method can reliably and with a good reproducibility detect any weak adhesive bond, either on metal or composite substrate.

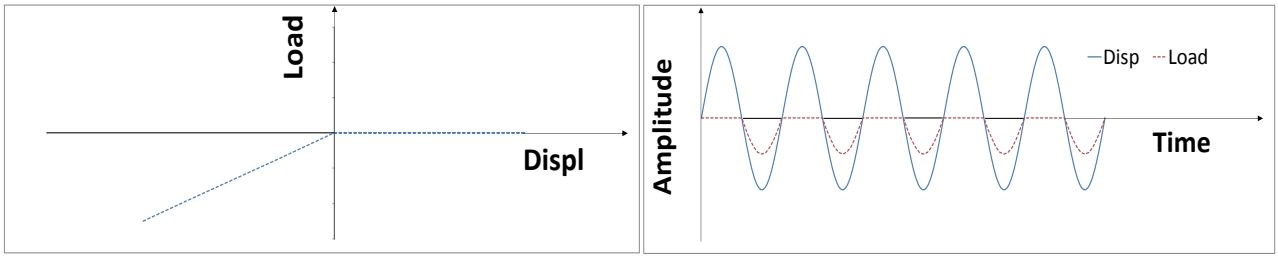

Figure 1. Nonlinearity induced by nonlinear load-displacement relation

Nevertheless, nonlinearities in the material response of a bonded joint structure undergone to harmonic excitation can be found. These nonlinear elastic phenomena are mainly due to the interaction between the propagating ultrasonic waves and the debonding region, which may lead to clapping conditions resulting in contact acoustic nonlinearities and in a nonlinear load-displacement relation (see Figure 1). The distorted ultrasonic waves transmitted through and/or reflected from a weak adhesive layer (that is a nonlinear interface) are commonly quantified in the frequency domain by the magnitude of harmonics of the input monochromatic frequency. Nonlinear dynamic systems also exhibit appearance of subharmonics in specific conditions. In general, nonlinear oscillation systems exhibit a greater variety of phenomena which result in the nonlinear spectrum transforms to subharmonics and chaos [10]. The acoustic subharmonics produced by the crack vibrations were observed [11, 12] and a subsequent threshold transition to chaotic dynamics for the higher excitations was shown [12, 13]. These results indicate the correlation between an integral damage induced and the subharmonic (and/or “acoustic noise”) level while they do not allow one to locate the flaws. In [14] it is demonstrated that besides the subharmonics, mechanical defects in solids, reveal a more general phenomenon of the self-modulation of vibrations that brings about a specific spectrum conversion. Furthermore, both the subharmonic and self-modulation spectral components feature a strong localization around the defect and provide reliable imaging of the damaged areas.

In this paper samples of single lap joints bonded by epoxy resin adhesives are extensively investigated experimentally and numerically, using Nonlinear Elastic Wave Spectroscopy (NEWS). With a fixed overlap of the two joined plates, two main configurations of samples were investigated, i.e. fully bonded and partially bonded. Experiments were performed exciting the samples with harmonic loading in the range between 10 kHz and 50 kHz. The spectral features of the response were investigated and interpreted by correlating the results with the numerical predictions of a finite element (FE) model aimed at representing the nonlinear material response generated by the interaction of the ultrasonic waves with the adhesive joint. Such a constitutive model uses a nonlinear user defined traction-displacement relationship

implemented by means of a cohesive material user model interface. Subharmonics and higher order harmonics were found in the structural response as a consequence of the nonlinearities of the samples behavior.

2. MATERIALS AND METHODS

The tested samples and the experimental set-up are shown in the following Figure 2.

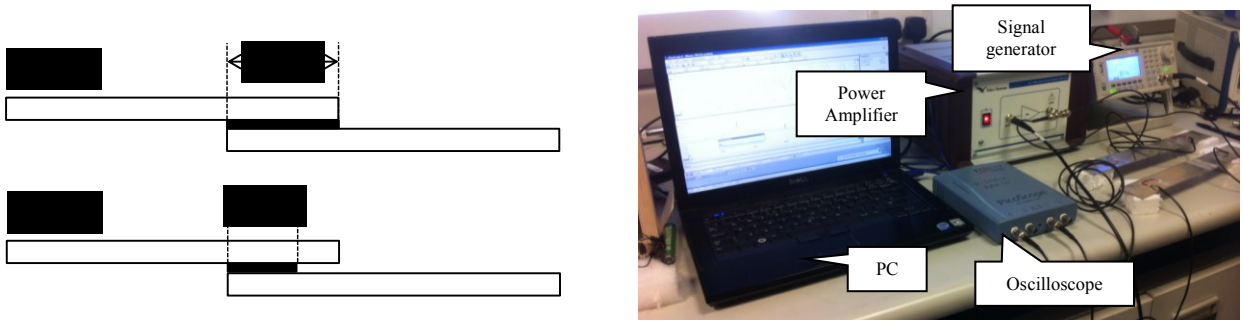

Figure 2. Test set-up

The single lap joint is formed by two plates 2 mm thick, 42 mm wide, 145 mm long, overlapped of 30 mm. The material of the plates is aluminum with the following mechanical properties: E = 71 GPa; density = 2770 kg/m^3; Poisson's ratio = 0.33. The adhesive is Araldic 320A with the following mechanical properties: E = 1.495 GPa, density = 1220 kg/m^3, Poisson's ratio = 0.3 and shear modulus G = 0.73 GPa. The nominal thickness of the adhesive layer is 0.15 mm. The experimental tests were aimed at characterizing the debonding by comparing the signals acquired by the piezo sensors (one transmitter sensor (S1) and one receiver sensor (S2)) surface bonded on the two samples. Two geometrically identical samples have been prepared, one labeled as Sample 1 (nominally fully bonded), the other one as Sample 2 (partially bonded). Debonding has been introduced by partially gluing the two plates (for Sample 2 the two plates are still overlapped of 30 mm but only 20 mm out 30 mm are bonded by the adhesive). The experimental procedure consisted of sending a pure harmonic signal through the signal generator linked to an amplifier in order to feed the exciting piezo sensor S1. The receiver sensor S2 was connected to an oscilloscope that allowed real-time acquisition of the propagating waveforms on a portable PC. The acquired signals were post-processed to detect the nonlinear elastic features using Matlab.

Higher Harmonics Generation

The equation of motion in linear elastodynamic can be obtained by combining the force equilibrium, Eq. (1), and the linear Hook's law, Eq. (2), in absence of body force and referring to Lagrangian coordinates x_j:

$$\frac{\partial \sigma_{ij}}{\partial x_j} = \rho \frac{\partial^2 u_i}{\partial t^2} \tag{1}$$

$$\sigma_{ij} = C_{ijkl} \varepsilon_{kl} \tag{2}$$

where σ_{ij} is the Cauchy stress tensor, u_i the displacement, ε_{kl} the strain, ρ the material density of and C_{ijkl} the fourth-order elasticity tensor. Assuming a longitudinal wave propagation along the x-direction the linear wave equation is:

$$\frac{1}{c_l^2} \frac{\partial^2 u(x,t)}{\partial t^2} - \frac{\partial^2 u(x,t)}{\partial x^2} = 0 \tag{3}$$

A solution of Eq. (3) as a plane wave oscillating with a harmonic frequency ω is:

$$u(x,t) = u_1 \sin(k_l x - \omega t) \tag{4}$$

$$u(0,t) = u_0\, sin(\omega t) = u_0\, sin(-\omega t) \tag{5}$$

where u_1 is the amplitude of the harmonic wave and k_l is the wave number equal to ω/c_l. Let assume a nonlinear elastic behavior of the material containing terms that describes "classical" nonlinearities (i.e. second and third order harmonics). Eq. (1) can be expressed as a power series of the strain in $\varepsilon_x = \partial u(x,t)/\partial x$ and combined to Eq. (2) yields:

$$\frac{\partial^2 u(x,t)}{\partial t^2} = {c_l}^2 \frac{\partial^2 u(x,t)}{\partial x^2}\left[1 + \beta \frac{\partial u(x,t)}{\partial x} + \frac{\gamma}{2}\left(\frac{\partial u(x,t)}{\partial x}\right)^2\right] \tag{6}$$

where $E = \partial\sigma_x/\partial\varepsilon_x$ is the linear elastic modulus, β and γ and d are higher order nonlinear elastic coefficients. To solve equation (6) the method adopted was a perturbation expansion of the displacement in the following form:

$$u(x,t) = u'(x,t) + v(x,t) = u'(x,t) + u''(x,t) + u'''(x,t) \tag{7}$$

where the contribution $|u'(x,t)| >> |v(x,t)|$ is the solution to the linear wave equation (3) expressed by (4). A first-order perturbation equation for the contribution $u''(x,t)$ is obtained substituting expression (7) in (6):

$$\begin{aligned} &\frac{\partial^2 u''(x,t)}{\partial t^2} - {c_l}^2 \frac{\partial^2 u''(x,t)}{\partial x^2} = {c_l}^2 \beta\left(\frac{\partial u'(x,t)}{\partial x}\right)\left(\frac{\partial^2 u'(x,t)}{\partial x^2}\right) \\ &= -\frac{{c_l}^2 \beta {k_l}^3 {u_1}^2}{2} sin\left[2(k_l x - \omega t)\right] \end{aligned} \tag{8}$$

for which a general solution has the form:

$$u''(x,t) = f(x) sin\left[2(k_x x - \omega t)\right] + g(x) cos\left[2(k_x x - \omega t)\right] \tag{9}$$

After some manipulations and after imposing the boundary conditions the solution becomes:

$$u''(x,t) = -\frac{\beta {k_l}^2 {u_1}^2}{8} x\, cos\left[2(k_l x - \omega t)\right] \tag{10}$$

where $u_2 = \frac{\beta {k_l}^2 {u_1}^2}{8} x$ is the amplitude of the second harmonic signal. Therefore, the nonlinear parameter β can be obtained experimentally by measuring the absolute amplitudes of the fundamental and the second harmonic signal:

$$\beta = 8 \frac{u_2}{{k_l}^2 {u_1}^2 x} \tag{11}$$

This process can be extended for the contribution $u'''(x,t)$ to the nonlinear wave equation as follows:

$$\begin{aligned} &\frac{\partial^2 u'''(x,t)}{\partial t^2} - {c_l}^2 \frac{\partial^2 u'''(x,t)}{\partial x^2} = {c_l}^2 \frac{\delta}{2}\left(\frac{\partial u'(x,t)}{\partial x}\right)^2\left(\frac{\partial^2 u'(x,t)}{\partial x^2}\right) \\ &= \frac{{c_l}^2 \gamma {k_l}^4 {u_1}^3}{8}\left\{-sin(k_l x - \omega t) - sin\left[3(k_l x - \omega t)\right]\right\} \end{aligned} \tag{12}$$

Substituting in the Eq. (12), the general form of the solution and imposing the boundary conditions on the third harmonic, the expression of the nonlinear parameter γ is obtained as the ratio between the third harmonic amplitude and the cubic amplitude of the fundamental pre-multiplied by a constant:

$$\gamma = 48 \frac{u_3}{{k_l}^3 {u_1}^3 x} \tag{13}$$

Subharmonics Generation

The equation of driven motion for a nonlinear oscillator can be used to derive the conditions for the subharmonic resonance generation in ultrasonic waves. This have the following general form:

$$\ddot{x} + 2\lambda\dot{x} + \omega_o^2 x + \varphi x^2 + \psi x^3 = \frac{F}{m} cos\, vt \tag{14}$$

where λ is a damping coefficient, ω_0 is a resonant frequency, φ and ψ are nonlinear parameters different from the classical ones, v is the excitation frequency, m is the mass. The solution of this equation may be sought as a harmonic function $x(t)=A(v)cos(vt)$ when the driving force F is reasonably small. For the superharmonic resonance the input frequency is taken as $\approx \omega_0/n$ and converted into ω_0 (resonant frequency) via the n-th nonlinearity of the oscillator. Using the perturbation approach, it is possible to find solutions to the (14) originating superharmonic resonance conditions [15]. Similarly, taking $v \approx n\omega_0$, the n-th approximation in (14) leads to subharmonic appearance conditions. Taking $v \approx 2\omega_0$, the second approximation in (14) yields:

$$\ddot{x}_2 + 2\lambda\dot{x}_2 + \omega_o^2\left[1 - \frac{2\varphi F}{3m\omega_0^4} cos\left[(2\omega_0 + \chi)t\right]\right]x_2 = 0 \tag{15}$$

which is a condition for a subharmonic (fundamental parametric) resonance (χ is a small quantity). In this case the solutions to (15) comprise unstable ultra-subharmonic outputs: $\omega_0 = pv/2$ (p = 1, 2, 3, …..).

3. EXPERIMENTAL RESULTS

In the following figures the main results related to Sample 1 (the nominally fully bonded one) and Sample 2 (the partially bonded one) are shown. In Figure 3, the normalized vibrational amplitude recorded by the receiver sensor at the excitation (fundamental) frequency during the experimental campaign is reported.

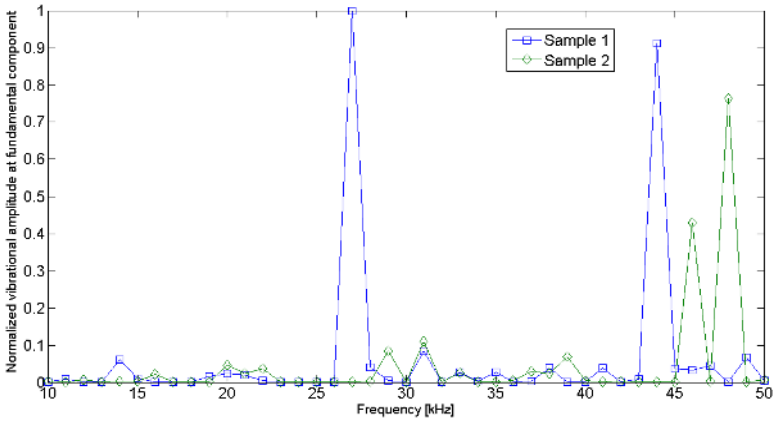

Figure 3. Fundamental component of the structural response for the two configurations investigated

This figure shows the structural linear response that was gradually changed by keeping constant the voltage amplitude. Although the linear response was measured only in one point of the structure, the first conclusion that can be drawn is that the dynamic behavior of the samples is very sensitive (as expected) to the adhesive extension that influences the vibrational modes of the specimens. Sample 1 exhibits clear peaks in the response at 27 kHz and 44 kHz, whilst sample 2 exhibits clear peaks at 46 kHz and 48 kHz. The structural response at different frequencies exhibit nonlinearities for both the Samples 1 and 2 (Figs. 4 and 5). This unexpected nonlinear behavior of sample 1 (that is nominally fully bonded) can be interpreted with defects inherent to the manufacturing process (voids, inclusions, non-uniformity of the adhesive layer, contact between the two plates, kissing bond and so on). Figures 4 and 5, according to Eqs. (11) and (13), report the evaluation of parameters β and γ characterizing the 2nd and 3rd order nonlinearities of the structural behavior of

the samples. These parameters have been widely used in nonlinear wave spectroscopy applications (for instance see [16-20]).

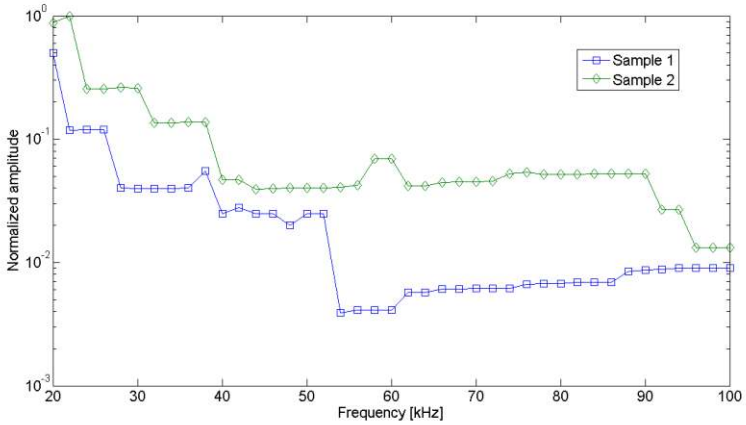

Figure 4. Parameter β evaluated in the frequency range of interest

The parameter β represents the importance of the second harmonic respect to the fundamental one: from Figure 4 it can be noticed that both samples exhibit nonlinear behavior resulting in the appearance of the second harmonic. This behavior is more pronounced at lower frequencies in the chosen range of interest. Sample 2 exhibits higher values of β than sample 1 as expected. Similarly, the parameter γ represents the importance of the third harmonic respect to the fundamental one and, also in this case, in the frequency range of interest, sample 2 exhibits higher values of γ than Sample 1.

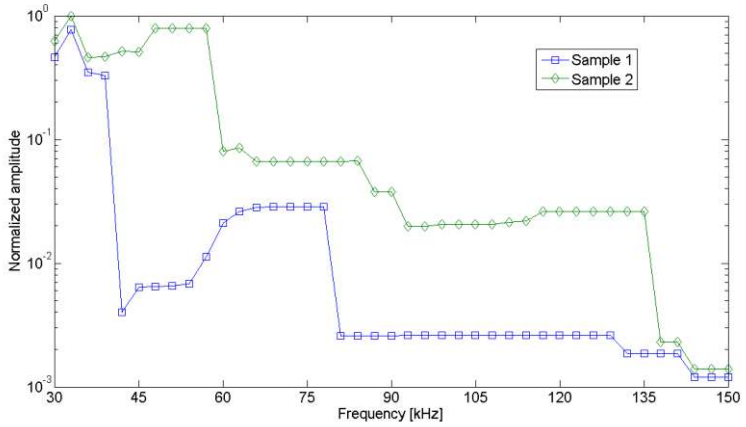

Figure 5. Parameter γ evaluated in the frequency range of interest

The structural response of both the samples is also characterized by the presence of subharmonics at half of the excitation frequency [see Eq. (15)]. In Figure 6, for both the configurations the normalized vibrational amplitude at f/2 components are reported for each excitation frequency. Sample 1 response exhibits clear peaks at 27 kHz, 35 kHz, 44 kHz, whilst sample 2 response exhibits clear peaks at 29 kHz, 32 kHz, 35 kHz, 46 kHz and 48 kHz.

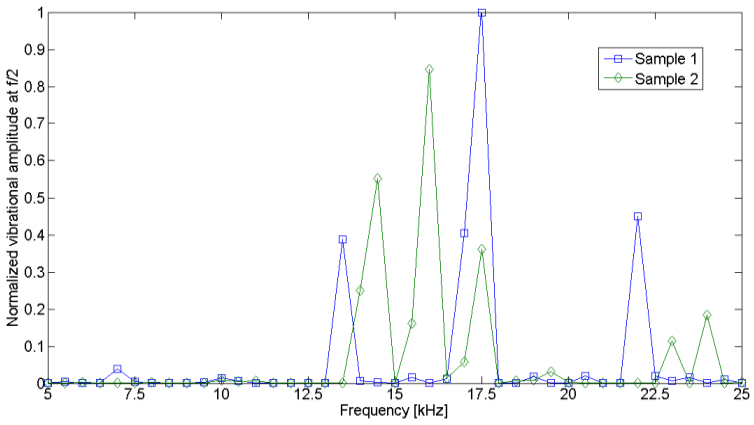

Figure 6. Subharmonic component (f/2) of the structural response for the two configurations investigated

In the following figures some Fast Fourier transform (FFT) signals are reported. Boundary conditions were carefully investigated to exclude that they could cause the appearance of subharmonics. It is concluded that subharmonics are due to poor adhesion leading to nonlinearities.

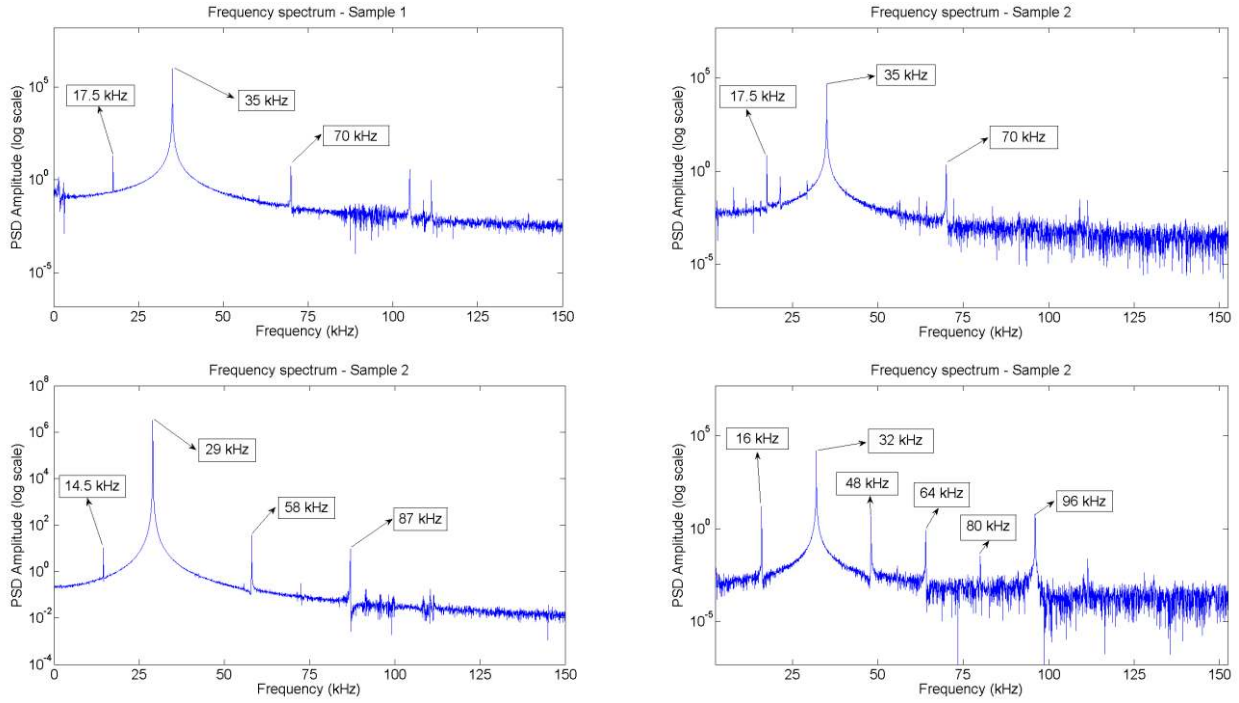

Figure 7. FFT at several frequencies of interest for sample 1 and sample 2

The FFTs reveal also the presence of second and third harmonics in the response. At 32 kHz, for the sample 2, the 16 kHz component leads also to the appearance of 48 KHz (3f/2) and 80 kHz (5f/2).

4. NUMERICAL MODEL

In the following section the results of numerical simulations based on a finite element model of the sample 2 are presented: the main target of these simulations was to investigate the dynamic behavior of the sample 2 in order to explain the appearance of subharmonics and higher order harmonics, by exploring the vibrational response due to the different modes in the frequency range of interest. If the vibrational mode shapes contributing to the dynamic response involve the adhesive and the adherends, exhibiting high levels of acceleration at the overlap, this can induce clapping conditions leading to the nonlinearities that appear clearly in the acquired signals.

A numerical model was devised and implemented using an explicit finite element solver LS-DYNA, for performing highly non-linear dynamic FE. Also, a user defined interface exists for the software which allows implementing various custom material, element, loading and failure models. In this study, a user defined cohesive material model was implemented. 3D dynamic FE model of two aluminum plates bonded with an adhesive was created: the finite element size depends on the wave propagation in 3D. The propagation velocity in a 3D-continuum medium of a dilatational wave is calculated as follows:

$$C_{3Dc} = \sqrt{\frac{E(1-\nu)}{(1+\nu)(1-2\nu)\rho}} \tag{16}$$

where E is Young's modulus, ν is the Poisson's ratio, and ρ is the specific mass density of the material. The FE code computes the smallest time step size by looping over all elements as follows:

$$\Delta t^{n+1} = a \times min\{\Delta t_1, \Delta t_2, \Delta t_3 \ldots . \Delta t_N\} \tag{17}$$

where N is the number of elements and a is a parameter usually chosen to be 0.9 or smaller due to numerical stability reasons. Central Difference numerical scheme is used as it is a conditionally stable explicit method requiring a Courant criterion to be met. The equation below is used by the FE code in order to estimate a critical time step, Δt_e, for solid elements.

$$\Delta t_e = \frac{L_e}{C_{3Dc}} \tag{18}$$

where C_{3Dc} is evaluated using Equation 16, while L_e is a characteristic length. In order to capture the wave propagation of a signal being sent at 35 kHz with a certain resolution, a sampling rate of 3.5 MHz was chosen. This leads to a time step size of approximately 0.3 μs. Subsequently, a minimum required characteristic length and hence the minimum element size was estimated using Equation 18, L_e = 1.8 mm. Subsequently, the geometry was meshed with 30660 finite elements. Figure 8 illustrates the FE mesh used for the analysis.

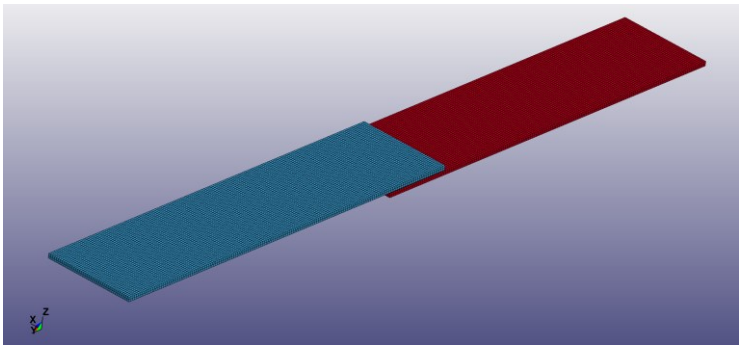

Figure 8. Finite element mesh of the single lap joint sample

In the physical experiment, the layer between the two aluminum plates was partially bonded with an adhesive. This region was modelled using cohesive elements. A cohesive element formulation connects via nonlinear spring elements the relative displacements between the upper and lower surface to a force per unit area; instead of strains, the deformation is in terms of the relative displacements between the upper and lower surfaces interpolated to the Gauss

point. The output of the material model is the force per unit area (i.e. traction) at the Gauss points, acting to oppose the displacement. Cohesive zone models (CZM) are typically used for analysis of bonded structures such composite panels in order to simulation a separation of two adjacent layers – i.e. delamination. However, the use of CZM in wave propagation and vibration studies is new. Using CZM in this study allowed modelling the geometry of the adhesive and the de-bonded region without a computational time penalty – cohesive elements are numerically efficient and can be of zero thickness or even become inverted without becoming unstable. In addition, the thickness of the cohesive elements has no effect on the time step calculation which is of high significance in terms of computational cost. One of disadvantages of this approach in the present study is the fact that the physics of the adhesive material are not modelled accurately; viscoelastic constitutive relationship would have been more appropriate. However, as the adhesive layer is comparatively very thin (approx. 0.15 mm), the inaccuracies in the constitutive relationship are assumed insignificant to the overall structural behavior in this case. A simple non-linear user defined traction-displacement relationship (Equation 19) was implemented by means of a cohesive material user model interface available as part of LS-DYNA User Defined package. This model was applied to the "de-bonded" region of the mesh.

$$F_N = 0 \text{ if } \delta_N \geq 0 \tag{19a}$$

$$F_N = E_N \delta_N \text{ if } \delta_N < 0 \tag{19b}$$

where F_N is traction (stress units) in normal direction, E_N and δ_N are the stiffness (stress/length units) and displacement normal to the plane of cohesive element respectively. Physically, the above relationship can be explained as an attempt to simulate a "clapping" phenomenon believed to occur in the debonded region. When the two surfaces are moving away from each other (i.e. positive displacement), the force is zero (i.e. no contact). When the surfaces move close together, the normal force takes a positive value simulating a contact.

In transient analysis, various frequencies were sent at the loading nodes (one frequency per simulation) for duration of 0.1 seconds. The range from 10 kHz to 50 kHz in steps of 5 kHz was explored. The results of post-processed nodal accelerations are plotted in Figure 9 and Figure 10. Higher harmonics (2f) are present on both the plots but have different amplitudes at the different frequencies. Sub-harmonic (f/2) is clearly identifiable only at 35 kHz. From the Figure 9 it is clear that at the different frequencies of excitation, the vibrational modes participating in the structural response are different and involve in different way the adhesive layer, leading to a more or less pronounced appearance of higher order harmonics, or determining the conditions of appearance of subharmonics.

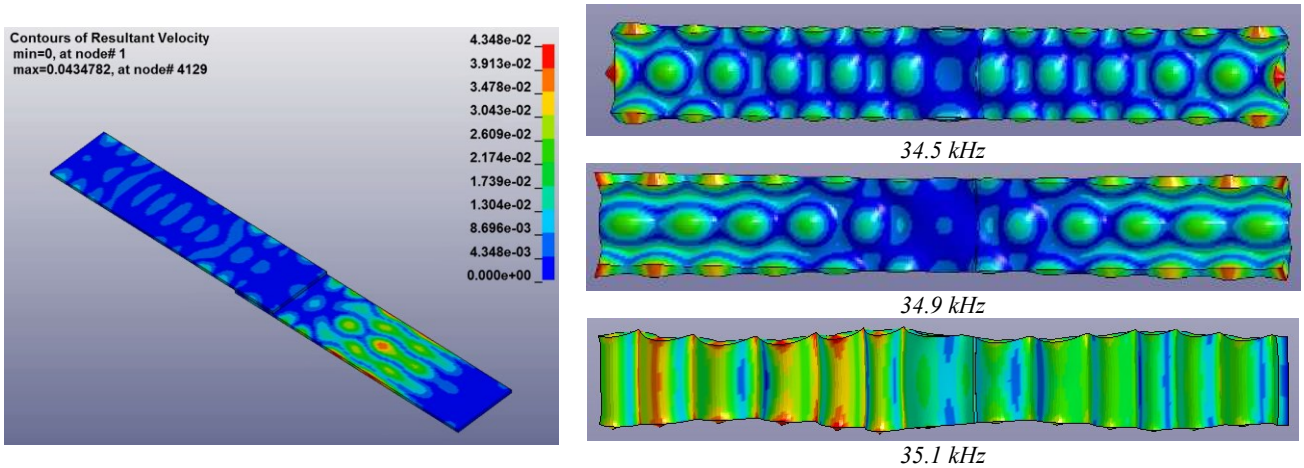

Figure 9. Snapshot of the nonlinear out-of-plane displacement from harmonic excitation and different modal shapes

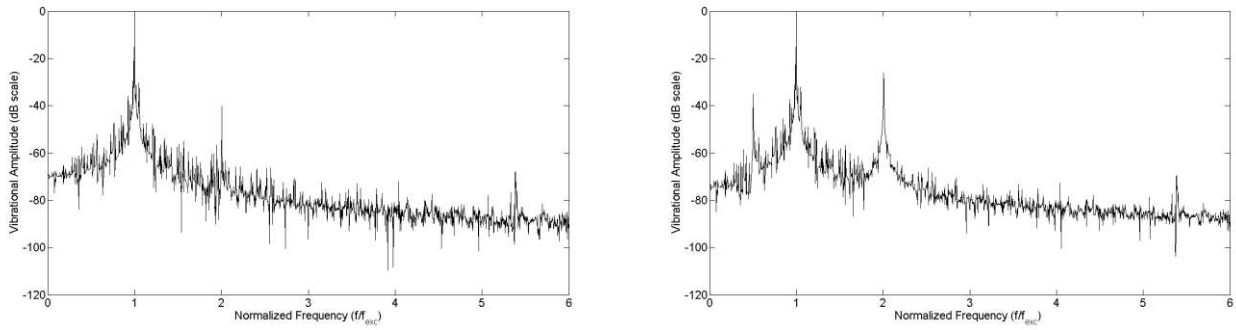

20 kHz *35 kHz*

Figure 10. FFT of the numerical acceleration

In this context, numerical models results are encouraging since they are able to clearly explain the nonlinearities of the structural response of the sample 2 (partially bonded sample). For what concerns the sample 1 (nominally fully bonded) nonlinear behavior, the explanation of defects in the manufacturing process gives just a direction of further investigation: on this matter, research activities are currently going on to understand properly the type and extent of the defects in the adhesive layer.

5. CONCLUSIONS

In this paper samples of nonlinear elastic response of single lap joints bonded by epoxy resin adhesives was experimentally and numerically investigated. Experimental testing were performed by exciting two different specimens with harmonic loading in the range between 10 kHz and 50 kHz. The spectral content of the acquired waveforms was investigated and interpreted by correlating the results with the numerical predictions of a nonlinear finite element (FE) model using a cohesive zone model (CZM) in order to represent the "clapping" condition. Subharmonics and higher order harmonics were found in the structural response as a consequence of the interaction of the propagating waves with the material nonlinear behavior. The use of nonlinear coefficients allowed evaluating the degree of nonlinearities of the two different samples and, as expected, the partially bonded one exhibited a higher degree of damage. Finally, the FE dynamic model confirmed the experimental results by providing numerical evidence of the appearance of subharmonics and higher order harmonics.

REFERENCES

[1] Guyott, C.C.H., Cawley P., Adams, R.D., "The non-destructive testing of adhesively bonded structure: a review", Journal of Adhesion, 20:129–159, (1986).

[2] Adams, R. D., Cawley P., "Defect types and non destructive testing techniques for composites & bonded joints", Construction and Building Materials, 3(4):170–183, (1989).

[3] Savage, G., "Failure prevention in bonded joints on primary load bearing structures", Engineering Failure Analysis, 14:321–348, (2007).

[4] Vine, K., Cawley, P., Kinloch, A. J., "The correlation of non destructive measurements and toughness changes in adhesive joints during environmental attack", Journal of Adhesion, 77(2):125–161, (2001).

[5] Jiao D., Rose, J.L., "An ultrasonic interface layer model for bond evaluation", Journal of Adhesion Science and Technology, 5(8):631–646 (1991).

[6] Vijaya Kumar, R.L., Bhat, M. R., Murthy, C.R.L., "Evaluation of kissing bond in composite adhesive lap joints using digital image correlation: Preliminary studies", International Journal of Adhesion & Adhesives, 42:60–68, (2013).

[7] Fucai Li et al., "Debonding detection using a self-calibration sensor network", Smart Materials and Structures, 19 (6), doi:10.1088/0964-1726/19/6/065007, (2010).

[8] Roach, D., Rackow, K., Duvall, R., "Innovative use of adhesive interface characteristics to non-destructively quantify the strength of bonded joints," 10th European Conference on Non-Destructive Testing (ECNDT10, Moscow, Russia), www.ndt.net, The NDT Database & e-Journal of Nondestructive Testing (2010).
[9] Ehrhart, B., et al., "Methods for the quality assessment of adhesive bonded CFRP structures-a resumé", Proceedings of 2nd International Symposium on NDT in Aerospace, (2010).
[10] Minorsky, N., [Nonlinear Oscillations], Van Nostrand, Princeton, (1962).
[11] Solodov, I.Yu., Korshak, B.A., "Instability, chaos and "memory" in acoustic-wave-crack interaction", Physical Review Letters, 88, 014303 (2002).
[12] Moussatov, A., Gusev, V., Castagnede, B., "Self-induced hysteresis for nonlinear acoustic waves in cracked material", Physical Review Letters, 90, 124301 (2003).
[13] Han, X., Li, W., Zeng, Zh., Favro, L.D., Thomas, R.L., "Acoustic chaos and sonic infrared imaging", Applied Physics Letter 81, 3188 (2002).
[14] Solodov, I., Wackerl, J., Pfleiderer, K., Busse, G., "Nonlinear self-modulation and subharmonic acoustic spectroscopy for damage detection and location", Applied Physics Letters 84, 5386, doi: 10.1063/1.1767283, (2004).
[15] Solodov, I. "Resonant acoustic nonlinearity of defects for highly-efficient nonlinear NDE", Journal of Nondestructive Evaluation, 33:252-262, (2014).
[16] Ciampa, F., Meo, M., "Nonlinear elastic imaging using reciprocal time reversal and third order symmetry analysis", Journal of Acoustical Society of America, 131 (6), 4316-4323, (2012).
[17] Ciampa, F., Pickering, S., Scarselli, G., Meo, M. "Nonlinear Damage Detection in Composite Structures using Bispectral Analysis", Proceedings of SPIE – The International Society for Optical Engineering, 906402-8, (doi:10.1117/12.2046631), (2014).
[18] Ciampa, F., Scarselli, G., Pickering, S., Meo, M., "Nonlinear Elastic Tomography using sparse array measurements", Proceedings of the 7th European Workshop on Structural Health Monitoring, 08 – 11 July 2014, Nantes, France.
[19] Ciampa, F., Onder, E., Barbieri, E., Meo, M., "Detection and Modelling of Nonlinear Elastic Response in Damage Composite Structures", Journal of Nondestructive Evaluation, doi: 10.1007/s10921-014-0247-7, (2014).
[20] Ciampa, F., Barbieri, E., Meo, M., "Modelling of Multiscale Nonlinear Interaction of Elastic Waves with three dimensional cracks", Journal of Acoustical Society of America, 135 (4), doi: 10.1121/1.4868476, (2014).